Dynamic Modeling and Motion Control of a Three-Link Robotic Manipulator

Jinho Kim, Andrew S. Lee, Kevin Chang, Brian Schwarz
Department of Mechanical Engineering, University of Maryland, Baltimore County (UMBC), 1000 Hilltop Circle, Baltimore, Maryland, USA, 21250

S. Andrew Gadsden
School of Engineering, University of Guelph, Guelph, Ontario, Canada, N1G 2W1

Mohammad Al-Shabi
Department of Mechanical Engineering, University of Sharjah, University City Rd, Sharjah, United Arab Emirates

E-mail: umbcjhkim@umbc.edu, alee20@umbc.edu, kevicha1@umbc.edu, schwarz4@umbc.edu, gadsden@uoguelph.ca, and malshabi@sharjah.ac.ae

Abstract

This paper presents the dynamic modeling and motion control of a three-link robotic manipulator, also known as the RRR robot. The Kinect motion capture system by Microsoft is used in conjunction with the manipulator. A camera is used to capture the motion of a user's arm and tracks certain angles made by parts of the arm. We consider a pinhole camera model to generate reference angles as per a pinhole camera model in our simulations. These desired angles are fed into the controller and are used by the RRR robot in an effort to copy the movement of the user. A proportional-derivative (PD) controller is developed and applied to the manipulator for improved trajectory tracking. The RRR robot manipulator is dynamically modeled and the results of the proposed control strategy demonstrate good trajectory following.

Keywords: Three-link robotic manipulator, System modeling, Motion capture, PD controller,

1. Introduction

Robotic manipulators have been developed and utilized in all sectors such as industry, medical, and military. Due to its potential to improve precision and enhance robustness, robotic manipulators have been applied to not only military missions but also medical devices in recent years. There are many research topics for medical devices with robotic manipulators such as human-robot collaboration, motion planning, and simultaneous control [1]-[4]. In the military field, we can easily perform robotic manipulator applications as well. For instance, autonomous ground vehicles with robotic manipulators are used in bomb disarming and reconnaissance. To conduct surgery or translate human movement with a robotic manipulator on military missions remotely, it is important to control the robotic manipulator according to operator's movement simultaneously [5]-[11].

In this paper, we consider controlling a system which consists of a camera and robotic manipulator. The pinhole camera model extracts reference angles from simulations in this paper. These desired angles are fed into the controller and are utilized by the robotic manipulator in an effort to mimic the movement of the user. A proportional-derivative (PD) controller is

designed and applied to the robotic manipulator for trajectory tracking.

This paper is organized as follows: in Section 2, the pinhole camera model is introduced and the modelling of three-link robotic manipulator is derived using the Euler-Lagrange equation. Based on that, a PD controller is designed in Section 3. Then, the simulation results are presented in Section 4.

2. Pinhole Camera Model

The pinhole camera model is used to obtain reference angles. The camera captures the user's arm motions, then the shoulder, elbow, and wrist angles are extracted through image processing.

The pinhole camera model is shown in Fig. 1. Here, we define $\mathbb{I}$ as the inertial coordinate frame, $\mathbb{C}$ as the camera frame, and $\mathbb{S}$ as the image frame. Then, let $[X_I, Y_I, Z_I]^T$ be the axes of the inertial coordinate frame $\mathbb{I}$, and $[X_{cam}, Y_{cam}, Z_{cam}]^T$ be the position vector in the camera frame $\mathbb{C}$. Let $[U_{image}, V_{image}]^T$ be the coordinate axes of the image frame $\mathbb{S}$ and O_S represents the principal point where the z-axis of the camera coordinate system intersects the image plane. The focal length of the camera, f, is the distance between O_{cam} and O_S. The mapping from a point $P = [x_c, y_c, z_c]^T \in \mathbb{C}$ onto the image plane can be written as Eq.(1).

$$p = \begin{bmatrix} u \\ v \end{bmatrix} = \frac{f}{z_c} \begin{bmatrix} x_c \\ y_c \end{bmatrix} \tag{1}$$

The user's arm is projected onto the image plane $\mathbb{S}$ through Eq.(1), then the three angles are calculated by extracting three points from the image plane using simple geometry. Let us define two points in $\mathbb{S}$ as $p_1 = (u_1, v_1)$ and $p_2 = (u_2, v_2)$. The angle can be calculated as follows;

$$\theta = \tan^{-1}\left(\frac{v_2 - v_1}{u_2 - u_1}\right) \tag{2}$$

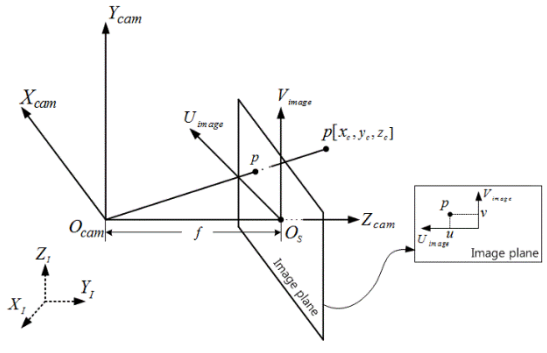

Figure 1. Geometry and coordinate frames for the pinhole camera model

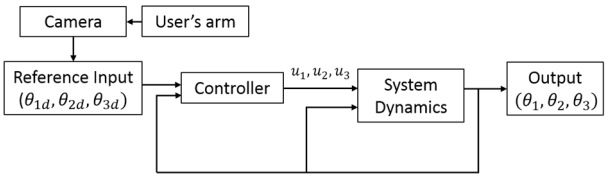

Figure 2. System Diagram

3. Dynamics and PD controller of Robotic Manipulator

In this section, we derive the dynamics of a three-link robotic manipulator and design a PD controller for it. The system diagram is depicted in Fig.2.

3.1. *Dynamics of robotic manipulator*

The configuration of the three-link robotic manipulator is shown in Fig.3. Here, θ_i $(i = 1,2,3)$ denotes the angles between each link, L_i is the length of the link, l_i is the distance from the centroid to corresponding axis, m_i is the mass, and J_i is the moment of inertia. Let τ_i denotes the joint torque and its counterclockwise rotation is assumed to be positive. Then, the Euler-Lagrange equation is applied as shown in Eq.(3)-Eq.(4) where $\mathcal{L}$ is the Lagrangian with kinetic energy $\mathcal{K}$ and potential energy $\mathcal{P}$ of the system [10].

$$\frac{d}{dt}\frac{\partial \mathcal{L}}{\partial \dot{\theta}_i} - \frac{\partial \mathcal{L}}{\partial \theta_i} = \tau_i \tag{3}$$

$$\mathcal{L} = \mathcal{K}_1 + \mathcal{K}_2 + \mathcal{K}_3 - \mathcal{P}_1 - \mathcal{P}_2 - \mathcal{P}_3 \tag{4}$$

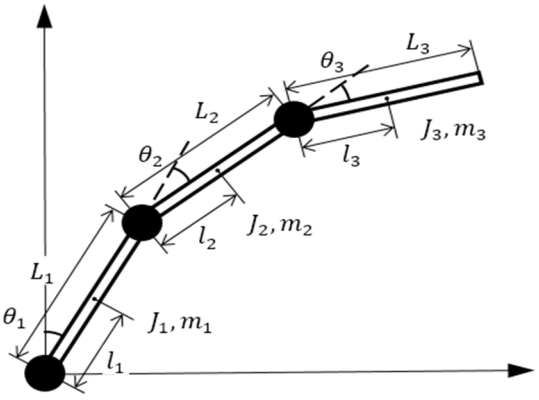

Figure 3. Configuration of the three-link robotic manipulator

In this system, $\mathcal{K}$ and $\mathcal{P}$ of each link can be written as per Eq.(5)-Eq.(6) where $\|v_i\|$ represents the magnitude of the velocity, $l_{i,y}$ is the position of the centroid that is dependent on joint coordinates.

$$\mathcal{K}_i = \frac{1}{2} m_i \|v_i\|^2 + \frac{1}{2} I_i \left(\sum_i \dot{\theta}_i\right)^2 \quad (5)$$

$$P_i = m_i g l_{i,y} \quad (6)$$

By these equations, we can obtain the final dynamics of the system in a simple form as the following:

$$u = M(\theta)\ddot{\theta} + C\left(\theta, \dot{\theta}\right) + g(\theta) \quad (7)$$

where $M(\theta)$ is the inertia matrix, $C\left(\theta, \dot{\theta}\right)$ represents the matrix of coriolis and centrifugal elements, $g(\theta)$ is the matrix of gravity elements, and, u is control input. The matrixes and its parameters can be written as follows:

$$M(\theta) = \begin{bmatrix} a_{11} & a_{12} & a_{13} \\ a_{12} & a_{22} & a_{23} \\ a_{13} & a_{23} & a_{33} \end{bmatrix},$$

$$C\left(\theta, \dot{\theta}\right) = \begin{bmatrix} b_1 \\ b_2 \\ b_3 \end{bmatrix},$$

$$g(\theta) = \begin{bmatrix} g_1 \\ g_2 \\ g_3 \end{bmatrix},$$

where,

$a_{11} = m_1 a_{c1}^2 + m_2(a_1^2 + a_{c2}^2 + 2a_1 a_{c2} c_2) + m_3(a_1^2 + a_2^2 + a_{c3}^2 + 2a_1 a_2 c_2 + 2a_1 a_{c3} c_{23} + 2a_2 a_{c3} c_3) + I_1 + I_2 + I_3$

$a_{12} = m_2(a_{c2}^2 + a_1 a_{c2} c_2) + m_3(a_2^2 + a_{c3}^2 + a_1 a_2 c_2 + a_1 a_{c3} c_{23} + 2a_2 a_{c3} c_3) + I_2 + I_3$

$a_{13} = m_3(a_{c3}^2 + a_1 a_{c3} c_{23} + a_2 a_{c3} c_3) + I_3$

$a_{22} = m_2 a_{c2}^2 + m_3(a_2^2 + a_{c3}^2 + 2a_2 a_{c3} c_3) + I_2 + I_3$

$a_{23} = m_3(a_{c3}^2 + a_2 a_{c3} c_3) + I_3$

$a_{33} = m_3 a_{c3}^2 + I_3$

$b_1 = -m_2 a_1 a_{c2}(2\dot{\theta}_1 + \dot{\theta}_2) s_2 \dot{\theta}_2 - m_3[a_1 a_2(2\dot{\theta}_1 + \dot{\theta}_2) s_2 + a_1 a_{c3}(2\dot{\theta}_1 + \dot{\theta}_2 + \dot{\theta}_3) s_{23} + a_2 a_{c3}(2\dot{\theta}_1 + 2\dot{\theta}_2 + \dot{\theta}_3) s_3]$

$b_2 = -m_2[a_1 a_{c2}(\dot{\theta}_1^2 + \dot{\theta}_1 \dot{\theta}_2) s_2 + a_1 a_{c2} \dot{\theta}_1 s_2 \dot{\theta}_2] - m_3[a_1 a_2(\dot{\theta}_1^2 + \dot{\theta}_1 \dot{\theta}_2) + a_1 a_{c3}(\dot{\theta}_1^2 + \dot{\theta}_1 \dot{\theta}_2 + \dot{\theta}_1 \dot{\theta}_3) s_{23} + a_2 a_{c3}(\dot{\theta}_1^2 + 2\dot{\theta}_1 \dot{\theta}_2 + \dot{\theta}_1 \dot{\theta}_3 + \dot{\theta}_2^2 + \dot{\theta}_2 \dot{\theta}_3) s_3 + a_1 a_2 \dot{\theta}_1 s_2 \dot{\theta}_2 + a_1 a_{c3} \dot{\theta}_1 \dot{\theta}_2 s_{23} + a_2 a_{c3}(2\dot{\theta}_1 + 2\dot{\theta}_2 + \dot{\theta}_3) s_3]$

$b_3 = -m_3[a_1 a_{c3}(\dot{\theta}_1^2 + \dot{\theta}_1 \dot{\theta}_2 + \dot{\theta}_1 \dot{\theta}_3) s_{23} + a_2 a_{c3}(\dot{\theta}_1^2 + 2\dot{\theta}_1 \dot{\theta}_2 + \dot{\theta}_1 \dot{\theta}_3 + \dot{\theta}_2^2 + \dot{\theta}_2 \dot{\theta}_3) s_3 + a_1 a_{c3} \dot{\theta}_1 \dot{\theta}_3 s_{23} + a_2 a_{c3}(\dot{\theta}_1 + \dot{\theta}_2) s_3 \dot{\theta}_3]$

$g_1 = g[c_1(m_1 a_{c1} + m_2 a_1 + m_3 a_1) + c_{12}(m_2 a_{c2} + m_3 a_2) + c_{123}(m_3 a_{c3})]$

$g_2 = g[(m_2 a_{c2} + m_3 a_2) c_{12} + m_3 a_{c3} c_{123}]$

$g_3 = g(m_3 a_{c3} c_{123})$.

3.2. *PD controller*

In this subsection, the PD controller for the three-link manipulator system is presented.

In order to control the system, τ_i can be defined as a control input u_i which controls θ_i with a reference input θ_r. The PD controller of the system are given by

$$u_i = k_{p,i} e_i + k_{d,i} \dot{e}_i \quad (8)$$

where k_p and k_d are proportional and derivative gains, respectively. The angle error, e_i, denotes $\theta_{r,i} - \theta_i$ and the derivative of the angle error, $\dot{e}_i$, denotes $\dot{\theta}_{r,i} - \dot{\theta}_i$.

4. Simulation Results

This section presents simulation results with initial parameters. The simulation used the initial settings which were defined as follows:

$$k_p = [37.5, 24.2, 16.4]$$

$$k_d = [1.34, 0.87, 1.04]$$

$$m_i = [1kg, 1kg, 1kg]$$

$$L_i = [0.2m, 0.2m, 0.2m], l_i = [0.1m, 0.1m, 0.1m]$$

$$J_i = [0.5kg \cdot m^2, 0.5kg \cdot m^2, 0.5kg \cdot m^2].$$

We generated movements of arm and extracted the shoulder, elbow, and wrist angles as reference inputs $\theta_{r,1}, \theta_{r,2}, \theta_{r,3}$. We set these reference inputs as the following:

$$\theta_{r,1} = 3\sin(0.1\pi t)$$

$$\theta_{r,2} = 4\cos(0.1\pi t)$$

$$\theta_{r,3} = 9\sin(0.15\pi t),$$

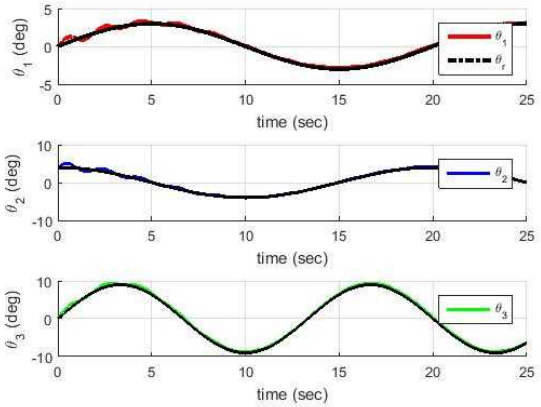

Figure 4. History of each angle. The black dashed lines are reference inputs and colored lines are current angles.

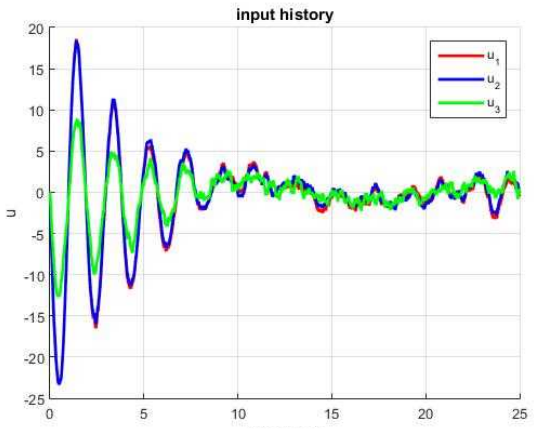

Figure 5. History of three inputs

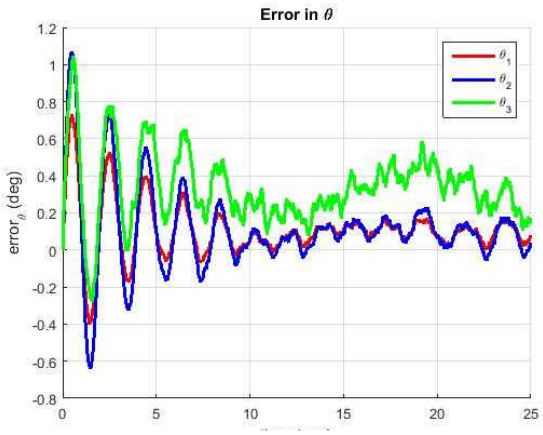

Figure 6. Errors between angles and reference inputs

where, t is time from 0 to 25 seconds in this simulation.

The history of each angle is shown in Fig.4 where the black dashed lines are reference inputs $\theta_{r,i}$ and colored lines are current angles. As shown in Fig.4, we can observe that the trajectories of the system angles follow the reference angels with satisfactory results. The initial overshoot in Fig.4 shows acceptable performance of the PD controller for this system.

Histories of the three inputs and errors between angles and reference inputs are shown in Fig.5 and Fig.6, respectively. From Fig.6, we confirm that errors have values less than one degree which is acceptable for a robotic manipulator with linkage dimensions similar to a human arm.

5. Conclusion

This paper presents a three-link robotic manipulator combined with a camera for capturing the user's motion. For the successful control of the system, the pin hole camera model captures the user's arm motion and extracts the shoulder, elbow, and wrist angles through image processing. Then, the dynamics of the system is derived and a PD controller is applied to control the angles of each link. The simulation results verified the efficacy of a PD controller showing satisfying results for tracking movement.

References

1. S. Najarian, M. Fallahnezhad, and E. Afshari, Advances in medical robotic systems with specific applications in surgery—A review, *Journal of medical engineering & technology*, 35(1) (2011) 19-33.
2. H. Jiang, J. P. Wachs, and B. S. Duerstock, Integrated vision-based robotic arm interface for operators with upper limb mobility impairments, *Proc. 2013 IEEE International Conference on Rehabilitation Robotics (ICORR),* (USA, Seattle, Jun. 2013), pp.1-6.
3. T. S. Lendvay, T. C. Brand, L. White, T. Kowalewski, S. Jonnadula, L. D. Mercer, D. Khorsand, J. Andros, B. Hannaford, and R. M. Satava, Virtual reality robotic surgery warm-up improves task performance in a dry laboratory environment: a prospective randomized controlled study, *Journal of the American College of Surgeons*,216(6) (2013): 1181-1192.
4. B. Hannaford, J. Rosen, D. W. Friedman, H. King, P. Roan, L. Cheng, D. Glozman, J. Ma, S. N. Kosari, and L. White. Raven-II: an open platform for surgical robotics research, *IEEE Transactions on Biomedical Engineering,* 60(4) (2013): 954-959.
5. X. Jian and L. Zushu, Dynamic model and motion control analysis of three-link gymnastic robot on horizontal bar, in *Proc. The 2003 IEEE International Conference on Robotics and Intelligent Systems and Signal Processing,* (China, Changsha, Oct. 2003).
6. I. David and G. Robles, PID control dynamics of a Robotic arm manipulator with two degrees of Freedom, *Control de Procesos y Robotica* (2012): 1-7.
7. B. Siciliano, S. Lorenzo, V. Luigi, and O. Giuseppe, *Robotics: modelling, planning and control,* (Springer Science & Business Media, 2010).
8. M.W. Spong, Swing Up Control of the Acrobot, in *Proc. The International Conference on Robotics and Automation,* (USA, San Diego, Oct. 1994), pp.2356-2361.
9. M.W. Spong, The swing up control problem for the acrobot, *IEEE Control System Magazine,* 15(1) (1995): 49-55.
10. M. W. Spong, S. Hutchinson, and M. Vidyasagar, *Robot modeling and control*, (Wiley, New York, 2006).
11. S. A. Gadsden, Smooth Variable Structure Filtering: Theory and Applications, *Ph.D. Thesis, McMaster*, 2011.